A support vector domain method for change detection in multitemporal images

F. Bovolo [a,*], G. Camps-Valls [b], L. Bruzzone [a]

[a] Dept. of Information Engineering and Computer Science, University of Trento, Via Sommarive, 38123 Povo, Italy
[b] Image Processing Laboratory (IPL), Universitat de València, Spain

ARTICLE INFO

ABSTRACT

This paper formulates the problem of distinguishing changed from unchanged pixels in multitemporal remote sensing images as a minimum enclosing ball (MEB) problem with changed pixels as target class. The definition of the sphere-shaped decision boundary with minimal volume that embraces changed pixels is approached in the context of the support vector formalism adopting a support vector domain description (SVDD) one-class classifier. SVDD maps the data into a high dimensional feature space where the spherical support of the high dimensional distribution of changed pixels is computed. Unlike the standard SVDD, the proposed formulation of the SVDD uses both target and outlier samples for defining the MEB, and is included here in an unsupervised scheme for change detection. To this purpose, nearly certain training examples for the classes of both targets (i.e., changed pixels) and outliers (i.e., unchanged pixels) are identified by thresholding the magnitude of the spectral change vectors. Experimental results obtained on two different multitemporal and multispectral remote sensing images demonstrate the effectiveness of the proposed method.

1. Introduction

In the remote-sensing literature, two kinds of approaches to change detection in multitemporal remote sensing images can be identified: the supervised and the unsupervised approach. The former requires ground truth information for setting up the system parameters, whereas the latter does not. Although supervised approaches usually result in higher change detection accuracies, unsupervised techniques are more appealing at an operational level as the ground truth information is not typically available in many change detection applications. In the literature, several unsupervised change detection methods have been proposed (Bazi et al., 2005; Bovolo and Bruzzone, 2005, 2006, 2007a,b; Bovolo et al., 2008; Bruzzone and Fernández Prieto, 2000; Ghosh et al., 2007; Inglada and Mercier, 2007; Radke et al., 2005; Singh, 1989). Among them, one of the simplest (yet effective) and most widely used technique is the change vector analysis (CVA) (Bovolo and Bruzzone, 2007b; Bruzzone and Fernández Prieto, 2000; Singh, 1989). CVA is typically applied to multispectral images acquired by passive sensors, by using all the spectral channels that contain useful information with respect to the considered kind of change. The CVA technique is based on three steps: (i) image comparison by vector subtraction; (ii) magnitude of the spectral change vectors computation (sometimes also the direction of SCVs is computed)

(Bovolo and Bruzzone, 2007b); and (iii) thresholding. The first step computes the vector difference of spectral feature vectors associated with pairs of corresponding pixels in two images acquired on the same geographical area at two different times, and results in a multispectral difference image. Each pixel in this image is associated with a multidimensional vector named spectral change vector (SCV). In the second step, the magnitude of each SCV is computed. This operation results in a 1-dimensional image usually referred as magnitude image. Finally, thresholding is applied to the magnitude image in order to obtain the desired change detection map. Due to the statistical behavior of multispectral images, and to the properties of the magnitude operator, it is possible to assert that pixels showing a magnitude higher than a given threshold value are changed, while pixels showing a magnitude lower than the threshold value are unchanged (Bovolo and Bruzzone, 2007b; Bruzzone and Fernández Prieto, 2000; Singh, 1989). A major drawback of using the magnitude of SCVs is that the magnitude operator is not biunique and results in a decrease of information with respect to the SCVs feature space. Nonetheless, if no ground truth is available, the magnitude operator allows one to establish a relatively simple criterion (based on thresholding) for identifying nearly certain pixels belonging to either the class of changed pixels or the class of unchanged pixels (Bovolo and Bruzzone, 2007b; Bovolo et al., 2008).

In this paper, in order to take advantage of the large amount of information present in the multispectral difference image, we formulate the change detection problem in the higher dimensional SCVs feature space. The unsupervised analysis of SCVs requires

* Corresponding author. Tel.: +39 0461 882056; fax: +39 0461 882093.
  E-mail address: francesca.bovolo@disi.unitn.it (F. Bovolo).
  URL: http://www.dit.unitn.it/rslab (F. Bovolo).

the application of clustering algorithms in the context of an *ill-posed* problem. In order to address this problem, we reformulate the unsupervised change detection problem in the multispectral difference image as a data domain description problem, also known as *one-class classification*. Among the different methods for domain description (or outlier detection) present in the literature (Ritter and Gallegos, 1997; Tarassenko, 1995), the support vector data description (SVDD) method (Tax and Duin, 1999, 2004) is adopted here. This method aims at mapping the data into a high dimensional feature space where a hypersphere that encloses most of the patterns belonging to the class of interest (*target class*) and rejecting the rest (*outliers*) can be defined. As all kernel methods, SVDD shows some interesting advantages over other techniques, like intrinsic regularization and robustness to noise and high dimensionality (Camps-Valls et al., 2007; Schölkopf et al., 1999; Schölkopf and Smola, 2002; Shawe-Taylor and Cristianini, 2004). SVDD was recently introduced in the remote-sensing literature (Muñoz-Marí et al., 2007; Camps-Valls et al., 2008) and demonstrated to be effective in solving classification and change detection problems when ground truth information is available. In both Muñoz-Marí et al. (2007) and Camps-Valls et al. (2008), SVDD is used as a *supervised* one-class classifier involving in the training phase only samples of the target class. In the present paper, the SVDD is included in a system for *unsupervised* change detection, that aims at separating pixels belonging to the class of change (*target class*) from all unchanged pixels (*outlier class*) without any ground truth information. In order to properly constrain the learning process in absence of ground truth information, an unsupervised procedure for identifying examples is adopted, which is based on a selective thresholding of the magnitude of SCVs (Bovolo et al., 2008). Thanks to the specific nature of the change detection problem, this approach leads to the identification of both positive and negative examples. The outlier seeds are included in the training of the SVDD leading to a more effective description of the change detection problem. The resulting one-class classifier (OCC) shows a higher capability in describing the target data (Ben-Hur et al., 2001; Tax and Duin, 1999, 2004).

The paper is organized into four sections. In the next section, the architecture of the proposed change detection method is presented and each of its components is described in detail. In section 3 experimental results obtained by applying the proposed technique to two different remote sensing data sets are presented. Finally, Section 4 draws the conclusion of this work.

2. Proposed methodology

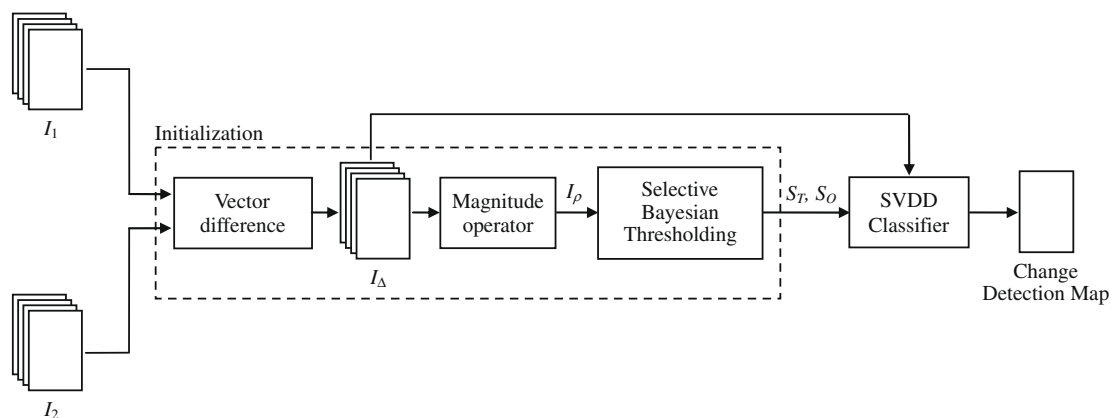Let I_1 and I_2 be two co-registered multispectral images of size $P \times Q$ acquired over the same geographical area at different times t_1 and t_2. Let N be the number of spectral channels of each considered image, and $\Omega = \{\omega_n, \omega_c\}$ the set of classes of no-changed and changed pixels to be identified, respectively. The proposed technique is based on a two-step procedure: (i) an initialization step that exploits a Bayesian thresholding of the magnitude of SCVs; and (ii) a support vector data description (SVDD) method that analyzes the multispectral difference image $I_\Delta = I_2 - I_1$ (see Fig. 1). Therefore, not only change information present in the magnitude of SVCs is considered, but also the high dimensional information present in the multispectral difference image. In the following, we analyze these steps in greater detail.

2.1. Bayesian initialization

The first step of the proposed unsupervised method for change detection aims at identifying the sets S_T and S_O of target (unchanged pixels) and outlier (changed pixels) patterns to be used as seeds for initializing the support vector data description (SVDD) one-class classifier (OCC). Following the discussion in (Bovolo et al., 2008), these subsets should contain pixels that are associated with changed and no-changed areas on the ground. However, as in our problem no ground truth information is available, the ideal assumption is relaxed and replaced with the more realistic constraint that seeds included in the sets S_T and S_O are associated with a high probability to belong to changed or unchanged areas.

According to the procedure described in (Bovolo et al., 2008), pixels with a high probability to belong to the change and no-change classes are identified by applying the CVA technique to I_1 and I_2, and by selectively thresholding the statistical distribution $p(i^\rho)$ of the magnitude of SCVs in I_ρ (i^ρ is the random variable associated with the magnitude of the spectral change vectors in I_ρ). In the literature, several threshold-selection methods (e.g., see Bruzzone and Fernández Prieto, 2000) have been proposed that can be used for identifying the threshold value T, which separates changed from unchanged pixels. Among them, we recall threshold-selection approaches based on the Bayesian decision theory, which showed to be effective in many change detection scenarios. The application of the Bayesian theory to threshold-selection requires the estimation of the statistical parameters of classes, i.e., the class prior probabilities and the class-conditional probabilities. As we are dealing with an unsupervised change detection problem, these statistical quantities are estimated from the data (without any prior information) according to the expectation-maximization (EM) algorithm (Bruzzone and Fernández Prieto, 2000). The estimated class-statistical parameters are then used with the Bayes decision rule for minimum-error for identifying the decision threshold T that separates changed from unchanged patterns. However, if we apply the Bayesian threshold to I_ρ, we obtain a

Fig. 1. Block scheme of the proposed method.

change detection map affected by the high uncertainty that characterizes patterns with a magnitude value close to the threshold. This problem arises from the loss of information associated with the magnitude operator. Nevertheless, the threshold value T represents a reasonable reference point for identifying the subsets S_T and S_O. According to this observation and following Bovolo et al. (2008), the desired sets of patterns with a high probability to be correctly assigned to one of the two classes are obtained by defining a margin around the minimum-error threshold. This margin conceptually separates uncertain from certain patterns. Patterns that fall outside the margin and show a high magnitude have a high probability to be changed and are labeled as targets, whereas patterns that fall outside the margin and show a low magnitude have a high probability to be unchanged and are labeled as outliers. Therefore, the resulting sets S_T and S_O are defined as (see Fig. 2):

$$S_T = \{\boldsymbol{x}_n \in \Re^N | i_n^\rho \geqslant T + \delta_2\}_{n=1}^{P \times Q} \quad \text{and}$$
$$S_O = \{\boldsymbol{x}_n \in \Re^N | i_n^\rho \leqslant T - \delta_2\}_{n=1}^{P \times Q} \tag{1}$$

where i_n^ρ is a 1-dimensional pattern in I_ρ, and $\boldsymbol{x}_n$ is a N-dimensional vector whose components are the spectral change vectors of the nth pattern in I_Δ. According to the standard classification setup, the nth target pattern in S_T is associated with a label $y_n = +1$, while the nth outlier pattern in S_O is associated with a label $y_n = -1$. It is worth noting that constants δ_1 and δ_2 should be selected in order to obtain a high probability that patterns in S_T and S_O are changed and unchanged, respectively.

2.2. Change detection based on SVDD including outlier information

The second step of the proposed method aims at giving a description of the class of changed pixels (*target*) in the SCVs feature space by exploiting the information present in the target and outlier sets defined in the previous step. The higher dimensionality that characterizes the multispectral difference image allows integrating the incomplete information on targets and outliers extracted from the 1-dimensional magnitude of SCVs and achieving a better description of the target class. The problem of finding a description of the target class data is faced here by using a support vector data description (SVDD) technique (Tax and Duin, 1999, 2004). SVDD aims at distinguishing between targets and outliers defining a closed boundary around the target data. In greater detail, the SVDD defines a minimum volume hypersphere in the kernel feature space that includes all (or most) of the target patterns available in the training set by minimizing a cost function.

Two different formulations of the cost function have been given in the literature. The first, and standard one, involves only target examples in the definition of the cost function (Tax and Duin, 1999); whereas, the second one involves both targets and outliers (Tax and Duin, 2004). It has been shown (Tax and Duin, 2004) that the joint use of both positive and negative examples in the training phase improves the data description. As in the considered data do-
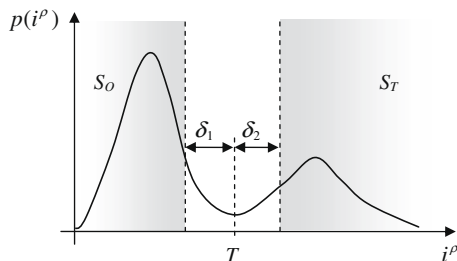
main description problem it is possible to generate examples of both classes (as described in the previous sub-section), we adopt the second formulation for the definition of the minimum enclosing ball.

Note that, depending on the size of the considered images, the cardinality of S_T and S_O can be high. To decrease the computational load, it is reasonable to randomly subsample both S_T and S_O. Therefore let us assume that after subsampling the set of target pixels is made up of K_T examples (i.e., $S_T = \{x_t\}_{t=1}^{K_T}$), whereas the set of outliers is made up of K_O counterexamples (i.e., $S_O = \{x_o\}_{o=1}^{K_O}$). In the following, indexes t and u will be used for identifying target patterns while indexes o and p will be used for identifying outliers. Let us assume that $\boldsymbol{x}_o$ and $\boldsymbol{x}_t$ in S_O and S_T, respectively, are column vectors. We can characterize the minimum enclosing ball (MEB) with its center $\boldsymbol{a}$ and radius R (>0), and define the problem of minimizing its volume as:

$$\min_{R,\boldsymbol{a}}\{R^2\} \tag{2}$$

subject to

$$\begin{cases} \|\phi(\boldsymbol{x}_t) - \boldsymbol{a}\|^2 \leqslant R^2 & \forall t = 1, \ldots, K_T \\ \|\phi(\boldsymbol{x}_o) - \boldsymbol{a}\|^2 > R^2 & \forall o = 1, \ldots, K_O \end{cases} \tag{3}$$

where $\varphi(\cdot)$ is a non-linear transformation that maps the input data into a high dimensional Hilbert feature space H where target data description can be achieved with a hypersphere. The first constraint in (2) comes from the assumption that positive examples should fall inside the sphere, whereas the second comes from the assumption that outliers should fall outside it (i.e., counterexamples should be rejected), see Fig. 3.

As for standard SVMs, the cost function can be reformulated in order to allow a certain amount of errors in both the positive and negative sample sets. Let us introduce *slack variables* ξ_t ($t = 1, \ldots, K_t$) and ξ_o ($o = 1, \ldots, K_o$) associated with the target and outlier patterns, respectively (see Fig. 3). Accordingly, the error function to be minimized becomes:

$$\min_{R,\boldsymbol{a},\xi_t,\xi_o} \left\{ R^2 + C_T \sum_{t=1}^{K_T} \xi_t + C_O \sum_{o=1}^{K_O} \xi_o \right\} \tag{4}$$

subject to

$$\begin{cases} \|\phi(\boldsymbol{x}_t) - \boldsymbol{a}\|^2 \leqslant R^2 + \xi_t, & \xi_t \geqslant 0, \quad \forall t = 1, \ldots, K_T \\ \|\phi(\boldsymbol{x}_o) - \boldsymbol{a}\|^2 > R^2 - \xi_o, & \xi_o \geqslant 0 \quad \forall o = 1, \ldots, K_O \end{cases} \tag{5}$$

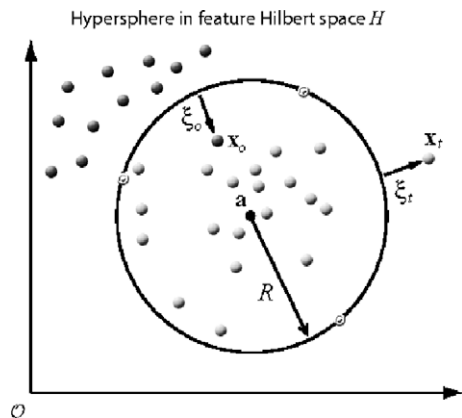Hypersphere in feature Hilbert space H

Fig. 3. An example of hyperspherical boundary defined by SVDD: light grey samples (inside the sphere) are targets; dark grey samples (outside the sphere) are outliers; samples on the boundary are support vectors. Both target and outlier samples on the wrong side of the boundary are associated with slack variables to deal with errors.

Fig. 2. Example of distribution of the magnitude of SCVs $p(i^\rho)$ and of the definition of the targets and outliers subsets.

where C_T and C_O are two regularization parameters that control the trade-off between the volume of the hypersphere and the number of rejected patterns for the target and outlier classes, respectively. The primal function (3) is usually solved through its Lagrange dual problem (Schölkopf and Smola, 2002; Tax and Duin, 2004), which reduces to the following minimization problem:

$$\max_{\alpha_t, \alpha_o} \left\{ \sum_{t=1}^{K_T} \alpha_t \langle \phi(\boldsymbol{x}_t), \phi(\boldsymbol{x}_t) \rangle - \sum_{o=1}^{K_O} \alpha_o \langle \phi(\boldsymbol{x}_o), \phi(\boldsymbol{x}_o) \rangle \right.$$
$$- \sum_{t,u=1}^{K_T} \alpha_t \alpha_u \langle \phi(\boldsymbol{x}_t), \phi(\boldsymbol{x}_u) \rangle + 2 \sum_{o=1}^{K_O} \sum_{t=1}^{K_T} \alpha_o \alpha_p \langle \phi(\boldsymbol{x}_o), \phi(\boldsymbol{x}_t) \rangle$$
$$\left. - \sum_{o,p=1}^{K_O} \alpha_o \alpha_p \langle \phi(\boldsymbol{x}_o), \phi(\boldsymbol{x}_p) \rangle \right\} \tag{6}$$

constrained to

$$\sum_{t=1}^{K_T} \alpha_t - \sum_{o=1}^{K_O} \alpha_o = 1$$

$$\boldsymbol{a} = \sum_{t=1}^{K_T} \alpha_t \phi(\boldsymbol{x}_t) - \sum_{o=1}^{K_O} \alpha_o \phi(\boldsymbol{x}_o) \tag{7}$$

$$0 \leqslant \alpha_t \leqslant C_T, \quad \forall t = 1, \ldots, K_T$$
$$0 \leqslant \alpha_o \leqslant C_O, \quad \forall o = 1, \ldots, K_O$$

The given data description always results in a closed boundary around the target class.

The inner product of mapping functions $\varphi(\cdot)$ (which are in principle unknown) that appears in (5) can be replaced with a kernel function $K(\cdot, \cdot)$:

$$K(\boldsymbol{x}_i, \boldsymbol{x}_j) = \langle \phi(\boldsymbol{x}_i), \phi(\boldsymbol{x}_j) \rangle \quad \text{with } i, j \in \{o, t, p, u\} \tag{8}$$

Substituting (7) into (5) we obtain

$$\max_{\alpha_t, \alpha_o} \left\{ \sum_{t=1}^{K_T} \alpha_t K(\boldsymbol{x}_t, \boldsymbol{x}_t) - \sum_{o=1}^{K_O} \alpha_o K(\boldsymbol{x}_o, \boldsymbol{x}_o) - \sum_{t,u=1}^{K_T} \alpha_t \alpha_u K(\boldsymbol{x}_t, \boldsymbol{x}_u) \right.$$
$$\left. + 2 \sum_{o=1}^{K_O} \sum_{t=1}^{K_T} \alpha_o \alpha_t K(\boldsymbol{x}_o, \boldsymbol{x}_t) - \sum_{o,p=1}^{K_O} \alpha_o \alpha_p K(\boldsymbol{x}_o, \boldsymbol{x}_p) \right\} \tag{9}$$

This allows us to construct a non-linear SVDD by defining only the kernel function, without the need to know the mapping $\varphi(\cdot)$ explicitly.

After solving the dual problem, to decide whether any vector $\boldsymbol{x}_n$ in I_Δ belongs to the class of change (*targets*) or no-change (*outliers*) the distance to the center of the sphere should be evaluated. A pattern $\boldsymbol{x}_n$ is classified as changed if it falls inside the sphere (i.e., its distance from the center of the sphere is lower than the radius), otherwise if the distance from the center of the sphere is higher than the radius, $\boldsymbol{x}_n$ falls outside the boundary and it is marked as unchanged. The decision rules becomes as follows:

$$x_n \in \begin{cases} \omega_c \leftrightarrow \|\phi(\boldsymbol{x}_n) - a\|^2 \leqslant R^2 \\ \omega_n \leftrightarrow \|\phi(\boldsymbol{x}_n) - a\|^2 > R^2 \end{cases} \tag{10}$$

In other words, a vector $\boldsymbol{x}_n$ is accepted as target (i.e., is classified as changed pixel) if the following inequality is satisfied:

$$\langle \phi(\boldsymbol{x}_n) - \boldsymbol{a}, \phi(\boldsymbol{x}_n) - \boldsymbol{a} \rangle$$
$$= K(\boldsymbol{x}_n, \boldsymbol{x}_n) - 2 \left[\sum_{t=1}^{K_T} \alpha_t K(\boldsymbol{x}_n, \boldsymbol{x}_t) - \sum_{o=1}^{K_O} \alpha_o K(\boldsymbol{x}_n, \boldsymbol{x}_o) \right]$$
$$+ \sum_{t,u=1}^{K_T} \alpha_t \alpha_u K(\boldsymbol{x}_t, \boldsymbol{x}_u) - 2 \sum_{o=1}^{K_O} \sum_{t=1}^{K_T} \alpha_o \alpha_t K(\boldsymbol{x}_o, \boldsymbol{x}_t)$$
$$+ \sum_{o,p=1}^{K_O} \alpha_o \alpha_p K(\boldsymbol{x}_o, \boldsymbol{x}_p) \leqslant R^2 \tag{11}$$

otherwise it is rejected and identified as outlier.

3. Experimental results

The proposed method has been tested on two multitemporal datasets made up of a pair of multispectral images acquired by the Thematic Mapper (TM) multispectral sensor of the Landsat-5 satellite. The first data set refers to an area in the Mexico, the second concerns the Sardinia Island (Italy). In the following subsections, we present the experimental setup and the results obtained on these data sets.

3.1. Experimental setup

In all the experiments the initialization threshold value T was obtained according to a manual-trial-and-error procedure (MTEP). The MTEP performs a non-automatic evaluation of the overall change detection errors versus all the possible values of the decision threshold; and then selects the threshold value that leads to a change detection map that shows the minimum overall error if compared to a reference map. This choice allowed us evaluating the performance of the proposed method without any bias due to human operator subjectivity or to the fact that the selection was made by an automatic thresholding algorithm. At an operational level, any automatic threshold-selection technique can be adopted (see Bruzzone and Fernández Prieto (2000) for more details about thresholding the magnitude image). The constants δ_1 and δ_2 were set equal to 10, resulting in S_T and S_O sets with a high cardinality. In order to reduce the computational load of the SVDD training, S_T and S_O were randomly sub-sampled. Several trials were carried out for different realizations of S_T and S_O. For both considered data sets the trials resulted in quite similar performance; therefore in the following only the results of the realization that exhibited in the highest Kappa accuracy are reported.

In the learning of the SVDD three parameters should be tuned: (i) the width σ of the employed Gaussian kernel function (Ritter and Gallegos, 1997); (ii) the regularization parameters C_T for wrong pixels in the target class; and iii) the regularization parameters C_O for wrong pixels in the outlier class. In our experiments, for convenience, we assumed that $C_T = C_O$. The selection process was based on a grid search strategy with values of the free parameters in the following ranges: (i) regularization parameters $C_T = C_O = C \in [10^{-3}, 5]$; and (ii) Gaussian kernel width $\sigma \in [0.01, 1]$. The tuning of C_T, C_O and σ was performed with both: (i) a supervised procedure based on the available reference map (this allows one to establish an "upper bound" of SVDD performance); and (ii) an unsupervised procedure based on the strategy proposed in (Bovolo et al., 2008) which is based on the information available in S_T and S_O and on a similarity measure between change detection maps obtained with different settings.

The results obtained with the proposed method were compared with the ones obtained with a standard CVA algorithm applied to I_ρ with manual trial-and-error thresholding procedure. The comparison is performed in terms of false alarms, missed alarms, overall errors and Kappa coefficient of agreement evaluated according to the reference maps.

3.2. Results on the Mexico data set

The Mexico data set is a section of 512×360 pixels of two co-registered multispectral images acquired by the TM sensor of the Landsat-5 satellite. The two images were acquired in April 2000 (I_1) and May 2002 (I_2) (Fig. 4a and b). Between the two acquisitions, two wildfires occurred in this area. A reference map concerning their location was available (Fig. 4c). This map includes 29,506 changed pixels and 154,814 unchanged pixels. A preliminary analysis pointed out that spectral channels 4 and 5 are the most rele-
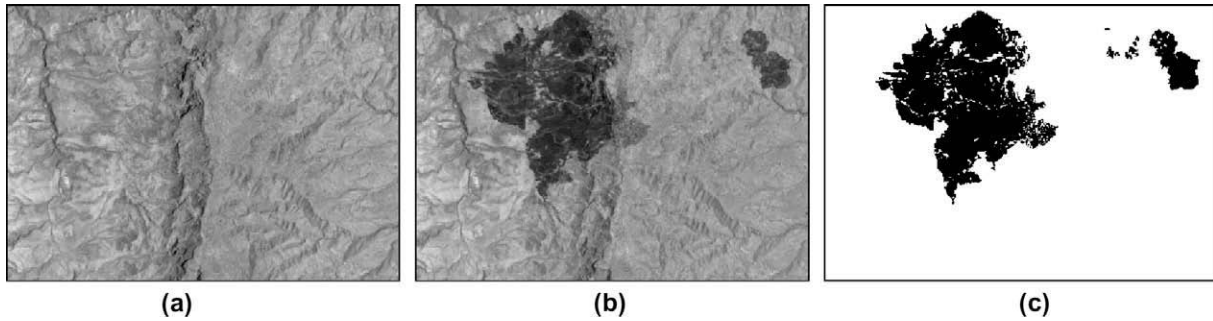
Fig. 4. Channel 4 of the Landsat-5 TM images acquired on the Mexico in: (a) April 2000, and (b) May 2002. (c) Available reference map of the burned areas.
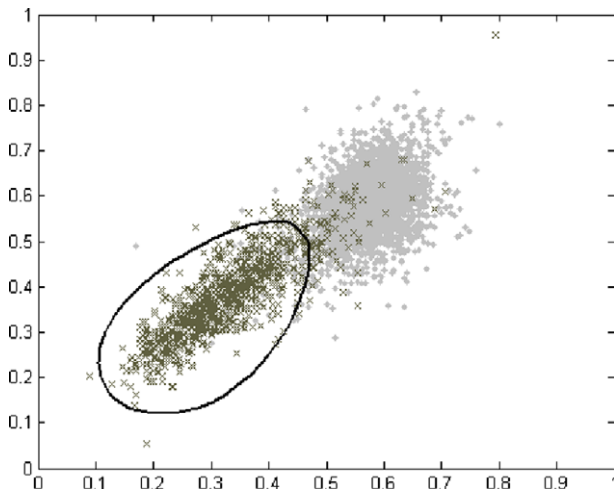

Fig. 5. Distribution of the class of changed (dark grey) and unchanged (light grey) pixels in the 2-dimensional I_Δ image according to the available reference map. The black line is the SVDD decision boundary obtained for the model selected in an unsupervised way according to the method proposed in (Bovolo et al., 2008) (Mexico data set).

vant for discriminating the burned area on this data set. Accordingly, we used these channels in our trials.

As can be seen from Fig. 5, this change detection problem is quite complex, as the target and outlier classes are significantly overlapped. In this critical situation the proposed technique resulted in higher change detection accuracy than the standard CVA technique (see Table 1). In greater detail, the proposed approach increased the estimated Kappa accuracy provided by the standard CVA from 0.844 to 0.903 (which in turn is quite similar to the estimated Kappa accuracy achieved with the unsupervised model selection procedure, i.e., 0.883). The improvement is associated to a slight decrease of false alarms (from 2428 to 2031) and to a sharp reduction of missed alarms (from 4801 to 3141). The unsupervised model selection strategy achieved results close to the ones obtained with the supervised model selection (which represent an upper bound for the operational use of the proposed method). Quantitative results are confirmed by a qualitative analysis of the change detection maps reported in Fig. 6.

3.3. Results on the Sardinia data set

The second data set is made up of two multispectral co-registered images acquired by the Thematic Mapper (TM) multispectral sensor of the Landsat-5 satellite on the Island of Sardinia (Italy) in September 1995 (I_1) and July 1996 (I_2). A section of 412×300 pixels including Lake Mulargia was selected for the experiments. As an example of the images used in the experiments, Fig. 7a and b show channel 4 of the September and July images, respectively. Between

Table 1
False alarms, missed alarms, overall errors and estimated Kappa coefficient associated with the change detection maps of the Mexico data set.

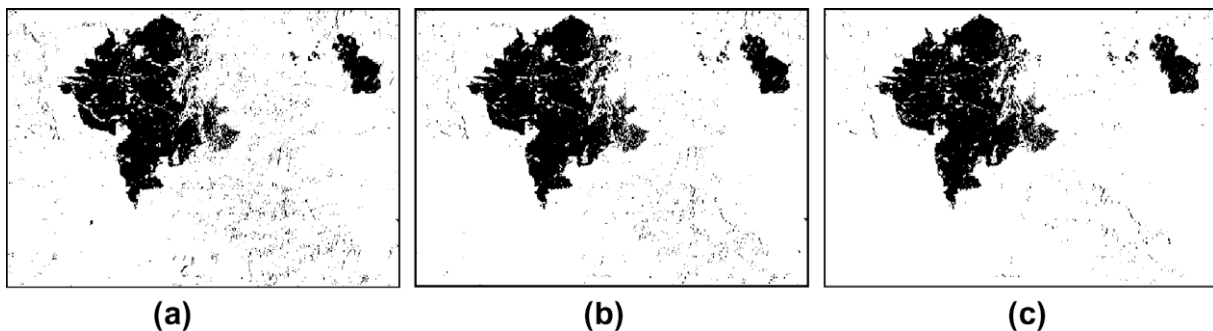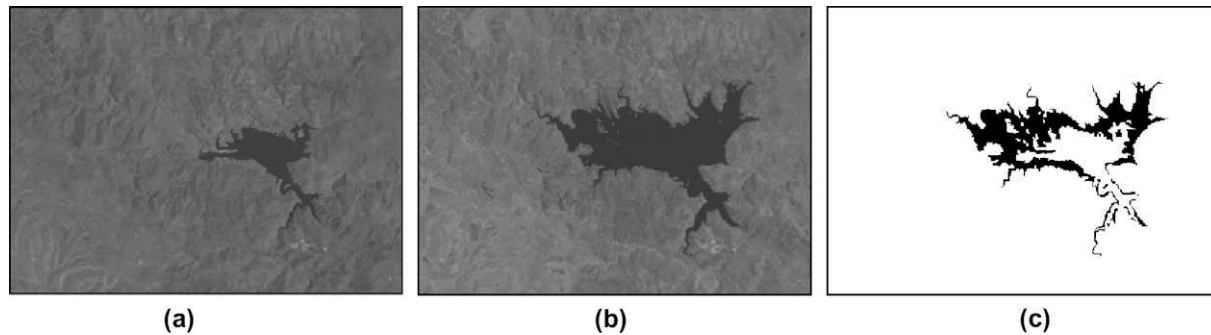| Technique		Missed alarms	False alarms	Overall error	Estimated Kappa statistic
Standard CVA		4801	2428	7229	0.844
Proposed SVDD	Supervised model selection	3141	2031	5172	0.903
	Unsupervised model selection	3135	2409	5544	0.883

Fig. 6. Change detection maps obtained for the Mexico data set with: (a) the standard CVA; (b) the proposed technique with unsupervised model selection; and (c) the proposed technique with supervised model selection (upper bound of method performance).

Fig. 7. Images of the Lake Mulargia (Italy). (a) channel 4 of the Landsat-5 TM image acquired in September 1995; (b) channel 4 of the Landsat-5 TM image acquired in July 1996; (c) available reference map of changed areas.

the two acquisition dates the lake surface registered an enlargement of the water surface resulting in a spectral change. A reference map of the analyzed site was defined according to a detailed visual analysis of both the available multitemporal images and the difference image. The obtained reference map contains 7480 changed pixels and 116,120 unchanged pixels (see Fig. 7c). In the experiments, we considered only the two spectral channels 4 and 7 of the TM, i.e., the near and the middle infrared, as they are the most reliable for detecting the considered change type.

The spectral signature of the water class significantly differs from the spectral signatures of all other natural classes. For this reason, SCVs associated with changes in the water class show smaller overlapping to unchanged SCVs than in the previous case in both the I_ρ and I_Δ images (see Fig. 8). Therefore detection of changes associated to the appearance (or disappearance) of water becomes a relatively simple problem. Under these conditions, the standard CVA performs well resulting in a high Kappa accuracy
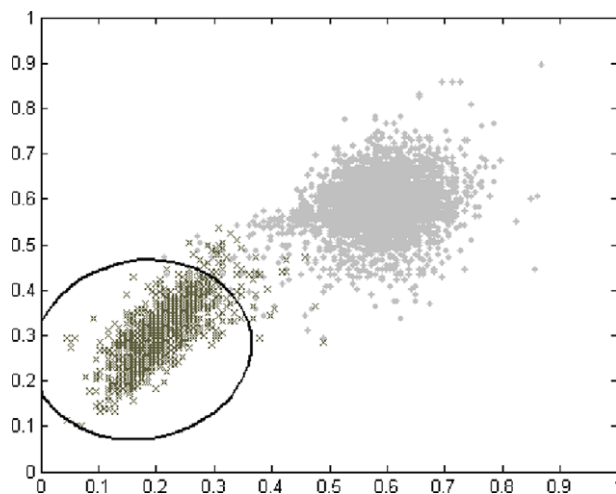
(i.e., 0.95), which is a result difficult to improve. Therefore, as expected, the proposed technique resulted in a similar Kappa accuracy (see Table 2). Nonetheless, it is worth observing that also in this case the CVA resulted in a slightly larger amount of false alarms (i.e., 369) than the proposed technique (i.e., 295 and 332, depending on the considered model selection strategy). This behavior is related to the higher sensitivity of the standard CVA technique to the presence of residual noise.

4. Discussion and conclusion

In this paper, a novel method for change detection based on CVA and SVDD has been proposed. The proposed method formulates the change detection problem as a minimum enclosing ball (MEB) problem with changed pixels as target objects. The MEB problem is solved after mapping spectral change vectors into a high dimensional Hilbert space. Once the minimum volume hypersphere is computed, it is mapped back into the original feature space where it results in a non-linear flexible boundary around target pixels. With respect to standard change vector analysis that considers only the 1-dimensional magnitude of SCVs, the proposed technique takes advantage from the higher amount of information present in the multidimensional SCVs feature space. This results in a better identification of changed areas, particularly in problems with overlapping classes. Furthermore, focusing on the changed pixels, it allows reducing the impact of residual registration noise in the final change detection map.

It is worth noting that the proposed change detection technique can be applied in a completely unsupervised framework performing the model selection of SVDD with the unsupervised approach presented in (Bovolo et al., 2008). As shown in the experimental section, unsupervised model selection demonstrated its validity resulting in a estimated Kappa accuracy close to the one achieved by the supervised approach to model selection (which represents an upper bound of performance for the proposed change detection method).

As future developments of the proposed work we propose to define a semi-supervised strategy for the learning of the SVDD parameters in order involve in the SVDD learning phase also unlabeled pixels according to the cluster assumption.

Fig. 8. Distribution of the class of changed (dark grey color) and unchanged (light grey color) pixels in the 2-dimensional I_Δ image according to the available reference map. The black line is the SVDD decision boundary obtained for the model selected in an unsupervised way according to the method proposed in (Bovolo et al., 2008) (Sardinia data set).

Table 2
False alarms, missed alarms, overall errors and estimated Kappa coefficient associated with the change detection maps of the Sardinia data set.

Technique		Missed alarms	False alarms	Overall error	Estimated Kappa statistic
Standard CVA		335	369	704	0.950
Proposed SVDD	Unsupervised model selection	362	332	694	0.950
	Supervised model selection	373	295	668	0.952

Acknowledgments

References

Bazi, Y., Bruzzone, L., Melgani, F., 2005. An unsupervised approach based on the generalized Gaussian model to automatic change detection in multitemporal SAR images. IEEE Trans. Geosci. Rem. Sens. 43 (4), 874–887.

Ben-Hur, A., Horn, D., Siegelmann, H.T., Vapnik, V., 2001. Support vector clustering. J. Mach. Learn. Res. 2, 125–137.

Bovolo, F., Bruzzone, L., 2005. A detail-preserving scale-driven approach to change detection in multitemporal SAR images. IEEE Trans. Geosci. Rem. Sens. 43 (12), 2963–2972.

Bovolo, F., Bruzzone, L., 2006. Unsupervised change detection in multitemporal SAR images. In: Chen, C. (Ed.), Signal and Image Processing for Remote Sensing. Taylor & Francis, Washington, DC.

Bovolo, F., Bruzzone, L., 2007a. A split-based approach to unsupervised change detection in large-size multitemporal images: Application to tsunami-damage assessment. IEEE Trans. Geosci. Rem. Sens. 45 (6), 1658–1670.

Bovolo, F., Bruzzone, L., 2007b. A theoretical framework for unsupervised change detection based on change vector analysis in polar domain. IEEE Trans. Geosci. Rem. Sens. 45 (1), 218–236.

Bovolo, F., Bruzzone, L., Marconcini, M., 2008. A novel approach to unsupervised change detection based on a semisupervised SVM and a similarity measure. IEEE Trans. Geosci. Rem. Sens. 46 (7), 2070–2082.

Bruzzone, L., Fernández Prieto, D., 2000. Automatic analysis of the difference image for unsupervised change detection. IEEE Trans. Geosci. Rem. Sens. 38, 1171–1182.

Camps-Valls, G., Gomez-Chova, L., Munoz-Mari, J., Rojo-Alvarez, J.L., Martinez-Ramon, M., 2008. Kernel-based framework for multitemporal and multisource remote sensing data classification and change detection. IEEE Trans. Geosci. Rem. Sens. 46 (6), 1822–1835.

Camps-Valls, G., Rojo-Álvarez, J.L., Martínez-Ramón, M., 2007. Kernel Methods in Bioengineering, Signal and Image Processing. Idea Group Inc., Harshey, PA (USA).

Ghosh, S., Bruzzone, L., Patra, S., Bovolo, F., Ghosh, A., 2007. A context-sensitive technique for unsupervised change detection based on Hopfield-type neural networks. IEEE Trans. Geosci. Rem. Sens. 45 (3), 778–789.

Inglada, J., Mercier, G., 2007. A new statistical similarity measure for change detection in multitemporal SAR images and its extension to multiscale change analysis. IEEE Trans. Geosci. Rem. Sens. 45 (5), 1432–1445.

Muñoz-Marí, J., Bruzzone, L., Camps-Valls, G., 2007. Evaluation of one-class domain description methods in remote sensing data classification. IEEE Trans. Geosci. Rem. Sens. 8, 2683–2692.

Radke, R.J., Andra, S., Al-Kofahi, O., Roysam, B., 2005. Image change detection algorithms: A systematic survey. IEEE Trans. Image Process. 14 (3), 294–307.

Ritter, G., Gallegos, M.T., 1997. Outliers in statistical pattern recognition and an application to automatic chromosome classification. Pattern Recognit. Lett. 18, 525–539.

Schölkopf, B., Smola, A., 2002. Learning with Kernels-Support Vector Machines, Regularization, Optimization and Beyond. MIT Press.

Schölkopf, B., Williamson, R.C., Smola, A., Shawe-Taylor, J., 1999. Support Vector Method for Novelty Detection. Advances in Neural Information Processing Systems 12. NIPS, Denver, CO.

Shawe-Taylor, J., Cristianini, N., 2004. Kernel Methods for Pattern Analysis. Cambridge University Press.

Singh, A., 1989. Digital change detection techniques using remotely-sensed data. Internat. J. Rem. Sens. 10, 989–1003.

Tarassenko, L., 1995. Novelty detection for the identification of masses in mammograms. In: Proc. 4th IEE Internat. Conf. on Artificial Neural Networks, vol. 4, pp. 442–447.

Tax, D., Duin, R.P., 1999. Support vector domain description. Pattern Recognit. Lett. 20, 1191–1199.

Tax, D., Duin, R.P., 2004. Support vector data description. Mach. Learn. 54, 45–66.